Parametric Analysis of Fluidized Bed using CFD

Siddayya Hiremath[1] M.R.Nagraj[2]
[1]M.Tech. Scholar [2]Professor
[1,2]Department of Mechanical Engineering
[1,2]Poojya Doddappa Appa College of Engineering Kalburgi, Karnataka, India

Abstract— In this project, we are studying the operating characteristics and design of fluidized bed cooling towers (FBCT), which may be used to cool hot water for industrial purposes. An analysis based on computational fluid dynamics is carried out for 1000 mm height and 150 mm diameter fluidized bed with different static bed heights of 200 mm, 300 mm and 400 mm with glass beads as solid particles of diameter 2.18mm. The software used for this assessment are Ansys design modeler for modeling the 2D geometry of the FBCT, Ansys meshing for meshing, Ansys fluent 14.5 as a solver and post-processor. Turbulence model used is k-epsilon, multiphase option used is Eulerian dense discrete phase multiphase model and water is sprayed through dense discrete phase model. The change in temperature of sprayed water and pressure drop of air is observed in all the three cases. Based on results it is observed that the static bed height of 300 mm is giving optimized results with maximum temperature drop and minimal pressure drop.

Key words: Fluidization, Ansys Fluent, Bed Height, Fluidization Time

I. INTRODUCTION

Gas–liquid–solid fluidized beds are used extensively in the refining, petrochemical, pharmaceutical, biotechnology, food and environmental industries. Some of these processes use solids whose densities are only slightly higher than the density of water. Gas–liquid–solid fluidized beds can be operated with different hydrodynamic regimes, which depend on the gas and liquid velocities, as well as the gas, liquid and solid properties. For proper reactor modeling, it is essential to know under which regime the reactor will be operating[1].

In a typical fluidized bed, solid particles are fluidized primarily by upward concurrent flow of liquid and gas, with liquid as the continuous phase and gas as dispersed bubbles if the superficial gas velocity is low. Because of the good heat and mass transfer characteristics, three-phase fluidized beds or slurry bubble columns have gained considerable importance in their application in physical, chemical, petrochemical, electrochemical and biochemical processing. Intensive investigations have been performed on three-phase fluidization over the past few decades; however, there is still a lack of detailed physical understanding and predictive tools for proper design, scale-up and optimum operation of such reactors. The calculation of hydrodynamic parameters in these systems mainly relies on empirical correlations or semi-theoretical models[2].

According to epstein , the liquid-supported solids operation characterizes fluidization with the liquid velocity beyond the minimum fluidization velocity; the bubble-supported solids operation characterizes fluidization with the liquid velocity below the minimum fluidization velocity where the liquid may even be in a stationary state. Countercurrent three-phase fluidization with liquid as the continuous phase, denoted as mode ii-a in figure-1, is known as inverse three-phase fluidization. Countercurrent three-phase fluidization with gas as the continuous phase, denoted as mode ii-b in figure-2, is known as a turbulent contact absorber, fluidized packing absorber, mobile bed, or turbulent bed contactor. In mode ii-a operation the bed of particles with density lower than that of the liquid is fluidized by a downward liquid flow, opposite to the net buoyant force on the particles, while the gas is introduced counter currently to that liquid forming discrete bubbles in the bed. In the mode ii-b operation (TCA operation), an irrigated bed of low-density particles is fluidized by the upward flow of gas as a continuous phase. When the bed is in a fully fluidized state, the vigorous moment of wetted particles give rise to excellent gas-liquid contacting. The gas and liquid flow rates in the TCA are much higher than those possible in conventional countercurrent packed beds, since the bed can easily exposed to reduce hydrodynamics resistances[3].

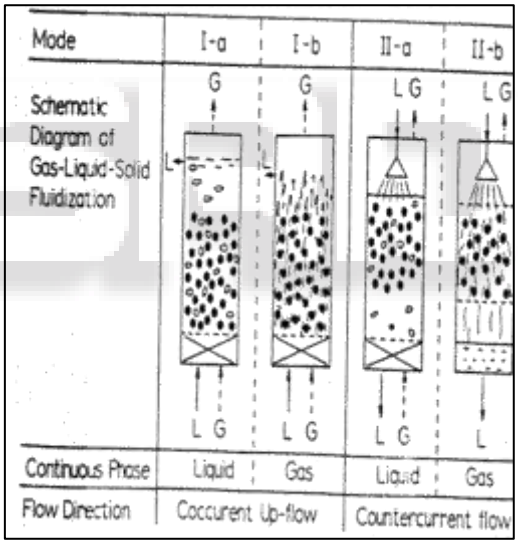

Fig. 1: Modes of operation of gas-liquid-solid fluidized bed

II. FLUIDISED BED COOLING TOWER OPERATION

Fluidization is the phenomenon by which the solid particles are made to behave like a fluid through contact gas or liquid or both. This principle is utilized in the development of three-phase fluidized bed cooling tower. At low flow rates of air the low density fluidizing solid particles lie on one another on a mesh or retaining grid at bottom of the cooling tower main body column as shown in *Fig a*. This state of fluidized bed is said to be in static or fixed state. If the velocity of the air flowing upward increases, Fluidization occurs, the low density bed materials forms as bubbles and intensive mixing of the bed materials and the air forms a turbulent action similar to a boiling fluid as shown in *Fig b*. This is the fluidized State. Further increase of the air velocity, will eventually cause entrainment of the fluidized bed particles from the column into the upward moving air.

The contact and close proximity of the particles to one another ceases as the solid particles become mobile as shown in *Fig c*. This is the pneumatic or hydraulic transport State[4].

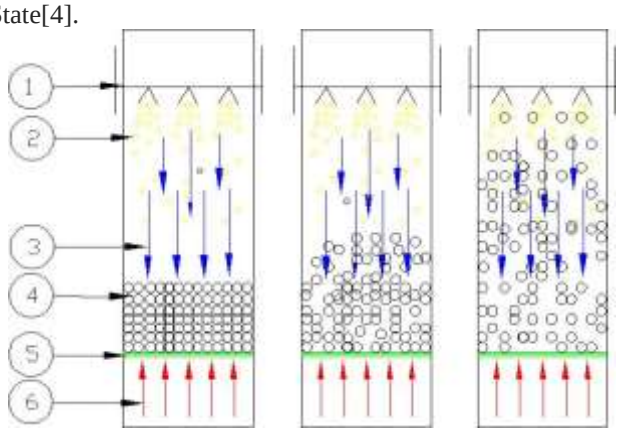

Fig. 2: three-phase fluidized beds

III. COMPUTATIONAL FLUID DYNAMICS

CFD is the science of predicting fluid flow, heat transfer, mass transfer, chemical reactions, and related phenomena by solving the mathematical equations which govern these processes using a numerical process. By means of computer based simulation. CFD is one of the branches of fluid mechanics that uses numerical methods and algorithms to solve and analyze problems that involve fluid flows computers are used to perform the millions of calculations required to simulate the interaction of fluids and gases with the complex surfaces used in engineering. However, even with simplified equations and high speed supercomputers, only approximate solutions can be achieved in many cases. More accurate codes that can accurately and quickly simulate even complex scenarios such as supersonic or turbulent flows are an ongoing area of research. The fundamental basis of any CFD problem is the Navier-stokes equations, which define any single-phase fluid flow. These equations can be simplified by removing terms describing viscosity to yield the Euler equations. Further simplification, by removing terms describing vorticity yields the full potential equations. CFD uses numerical methods to solve these fundamental nonlinear differential equations for pre-defined geometries and boundary conditions to linearized form. The result is a wealth of predictions for flow velocity, temperature, and phase hold up, pressure etc for any regions where flow occurs. The result of CFD analysis is relevant engineering data which are used in conceptual studies of new designs, detailed product development, troubleshooting, and design.[5]

A. Equations

Continuity equation:

$$\frac{\partial}{\partial t}(\varepsilon_k \rho_k) + \nabla(\rho_k \varepsilon_k \vec{u}_k) = 0$$

Where ρ_k is the density and ε_k is the volume fraction of phase k=g, s, l and the volume fraction of the three phases satisfy the following condition:

$$E_g + \varepsilon_l + \varepsilon_s = 1$$

B. Momentum Equations:

Where p is the pressure and μ_{eff} is the effective viscosity. The second term on the r.h.s of solid phase momentum equation is the term that accounts for additional solid pressure due to solid collisions. The terms $m_{i,l}$, $m_{i,g}$, and $m_{i,s}$ of the above momentum equations represent the inter phase force term for liquid, gas and solid phase, respectively.

For liquid phase:

$$\frac{\partial}{\partial t}(\rho_l \varepsilon_l \vec{u}_l) + \nabla(\rho_l \varepsilon_l \vec{u}_l \vec{u}_l) = -\varepsilon_l \nabla P + \nabla(\varepsilon_l \mu_{eff,l}(\nabla \vec{u}_l + (\nabla \vec{u}_l)^T)) + \rho_l \varepsilon_l g + M_{i,l}$$

For gas phase:

$$\frac{\partial}{\partial t}(\rho_g \varepsilon_g \vec{u}_g) + \nabla(\rho_g \varepsilon_g \vec{u}_g \vec{u}_g) = -\varepsilon_g \nabla P + \nabla(\varepsilon_g \mu_{eff,g}(\nabla \vec{u}_g + (\nabla \vec{u}_g)^T)) + \rho_g \varepsilon_g g - M_{i,g}$$

For solid phase:

$$\frac{\partial}{\partial t}(\rho_s \varepsilon_s \vec{u}_s) + \nabla(\rho_s \varepsilon_s \vec{u}_s \vec{u}_s)$$

IV. METHODOLOGY

The problem consists of a three phase fluidized bed in which air and liquid (water) enters at the bottom of the domain. The bed consists of solid material (glass beads) of uniform diameter which forms a desired height in the bed.

Phases	Density	Viscosity
Air	1.225 kg/m^3	1.789*10^{-05} kg/m-s
Water	998.2 kg/m^3	0.001003 kg/m-s
Glass beads	2470 kg/m^3	0.001003 kg/m-s

Table 2: Properties of air, water and glass beads used in experiment

A. Turbulence Modeling:

Additional transport equations for the turbulent kinetic energy k and its dissipation rate ε were considered: the realizable k–ε model was chosen for modelling the turbulence. It joins the properties of the standard k–ε model, such as robustness and reasonable accuracy for a wide range of industrial applications, with recently developed model improvements that provide better performance in the presence of jets and mixing layers. The upgrading concerns the formulation of the turbulent viscosity and the transport equation for ε [6].

K–ε models assume a high Reynolds number and fully turbulent flow regime so auxiliary methods are required to model the transition from the thin viscous sub-layer flow region along a wall to the fully turbulent, free stream flow region. The choice of the standard walls function approach determines that the viscosity affecting the near-wall region is not resolved. Instead, analytical expressions are used to bridge the wall boundary and the fully turbulent flow field: the expression implemented in fluent is the logarithmic law of the wall for velocity; corresponding relations are available for temperature and wall heat flux. Wall functions avoid the turbulence model adaptation to the presence of the wall, saving computational resources.[7]

B. Geometry and Mesh

The first step in CFD simulation of fluidized bed column is preprocessor, which has been done by dm tool, to design the problem in geometrical configuration and mesh, the geometry is done by using Ansys design modeler and meshing in Ansys meshing. Before fluid flow problems can be solved, fluent needs the domain in which the flow takes

place to evaluate the solution. The flow domains have been created in dm which as shown in fig3 and fig4. Below in 2D geometry quad meshing has been done with element type quad.

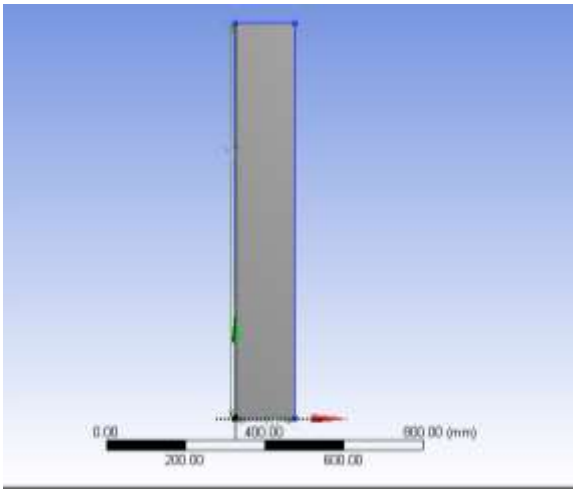

Fig. 3: 2D model of fluidized bed cooling tower

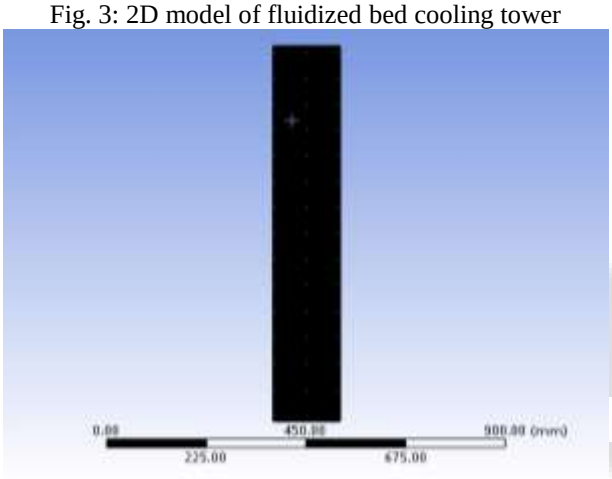

Fig. 4: 2D quadrilateral mesh

C. Boundary and Initial Conditions

In order to obtain a well-posed system of equations, reasonable boundary conditions for the computational domain have to be implemented. Inlet boundary condition is a uniform gas velocity at the inlet and outlet boundary condition is the pressure boundary condition, which is set as 101325 pa. Wall boundary conditions are no-slip boundary conditions for air and liquid phase. For patching a solid volume fraction, the solid in the part of the column up to which the glass beads were initially fed has been used. At initial condition the solid volume fraction of 0.60 of the static bed height of column has been used.

V. RESULTS AND DISCUSSION

A. Case 1: Fluidized Bed with Static Bed Height of 200 Mm.

The simulated results of fluidized bed system investigated has been presented in this chapter. Contours of volume fraction of solid with respect to time in simulation has been shown in fig 5. With the inlet air velocity 0.125 m/s for 1 m height column, the initial solid bed height of 200 mm and glass beads of size 2.18 mm has been used. The volume fraction of solid at different time steps has been shown below.

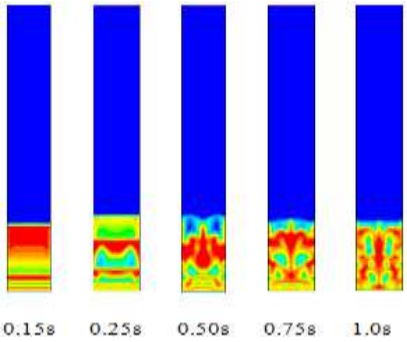

Fig. 5: Fluidization of solids

1) Volume Fraction of Air

Figure 6 shows the contours of volume fraction of air where blue color indicates low volume fraction of air and red color shows the maximum volume fraction of air. Wherever blue color is present it indicates air is less and solids are present at that spot. And red color indicates there is no solid at that spot.

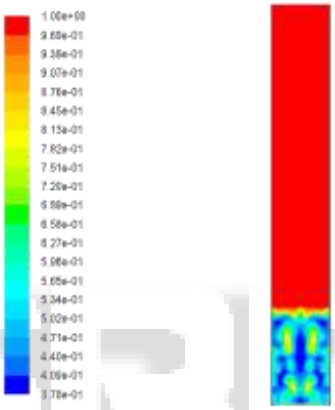

Fig. 6: The volume fraction of air in fluidized bed after fluidization

2) Temperature Contours of Water

From fig7, it is observed that temperature of water sprayed initially is at 315k.Water moves from top to bottom, temperature reduces gradually till the bottom of bed and at the bottom of the bed is 300k to 302k.

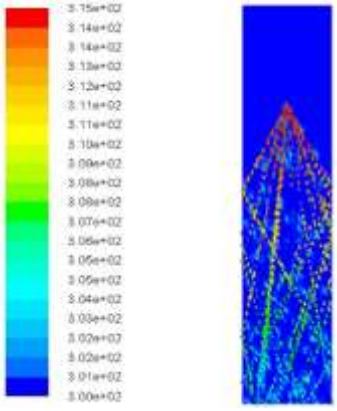

Fig. 7: Decrease of water temperature as it passes through fluidized bed.

3) Pressure Contours

Following Figure 8 shows the total pressure contour of 20 cm bed height. From fig it is seen that at the bottom of bed maximum pressure is noted which of the order of $3.02X10^{3}$ Pa. As bed height increases, gradually pressure decreases from $3.02X10^{3}$pa to $1.51X10^{2}$pa and it reaches a constant pressure value of $8.07X10^{-3}$ till the of the bed column. The

average pressure at the Inlet is 2950 Pascal and at the outlet average pressure is 0.00807 Pa. This gives a pressure drop of 2950 Pa.

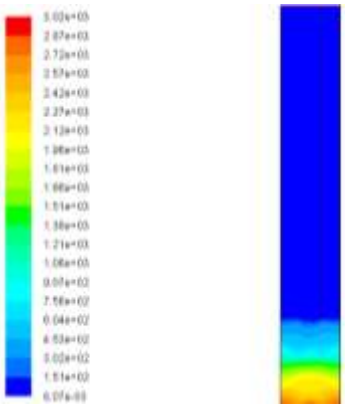

Fig. 8: Pressure distribution of air in Pascal for static bed height of 200 mm

B. Case 2: Static Bed Height of 300 mm.

The simulated results of fluidized bed system investigated have been presented in this chapter. Contours of volume fraction of solid with respect to time in simulation has been shown in fig8. With the inlet air velocity 0.125 m/s for 1 m height column, the initial solid bed height of 300 mm and glass beads of size 2.18 mm has been used. The volume fraction of solid at different time steps has been shown in below fig9.

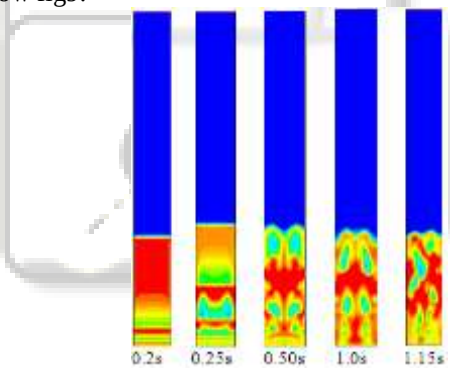

Fig. 9: Fluidization with static bed height of 300 mm.

1) Volume fraction of air

Figure 10 shows the contours of volume fraction of air where blue color indicates low volume fraction of air and red color shows the maximum volume fraction of air. Wherever blue color is present it indicates air is less and solids are present at that spot. And red color indicates there is no solid at that spot.

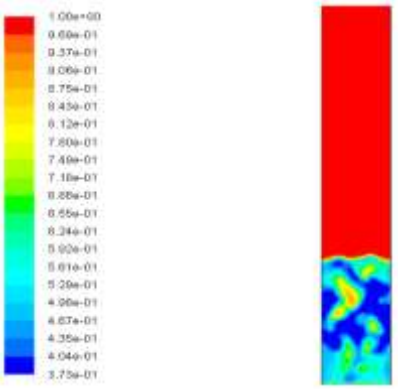

Fig. 10: The volume fraction of air in fluidized bed after fluidization.

2) Temperature Contours of Water

From fig11, it is observed that temperature of water sprayed initially is at 315k.Water moves from top to bottom, temperature reduces gradually till the bottom of bed and at the bottom of the bed is 298k to 300k.

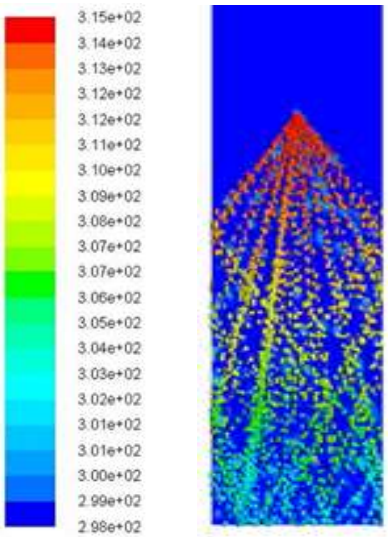

Fig. 11: Water temperature distribution as it passes through the fluidized bed.

3) Pressure Contours

Following Figure 12 shows the total pressure contour of 30 cm bed height. From fig it is seen that at the bottom of bed maximum pressure is noted which of the order of $4.03X10^3$ Pa. As bed height increases, gradually pressure decreases from $4.03X10^3$pa to $2.02X10^2$ pa and it reaches a constant pressure value of $5.38X10^{-3}$ till the of the bed column. The average pressure at the Inlet is 3950 Pascal and at the outlet average pressure is 0.00538 Pa. This gives a pressure drop of 3950 Pa

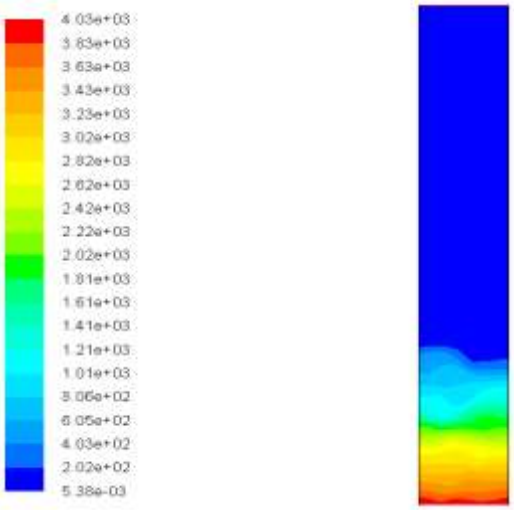

Fig. 12: Pressure distribution for static bed height of 300mm

C. Case 3: Static bed height 400 mm

The simulated results of fluidized bed system investigated has been presented in this chapter. Contours of volume fraction of solid with respect to time in simulation has been shown in fig13. With the inlet air velocity 0.125 m/s for 1 m height column. For this case the initial solid bed height of 400 mm and glass beads of size 2.18 mm has been used. The volume fraction of solid at different time steps has been shown below.

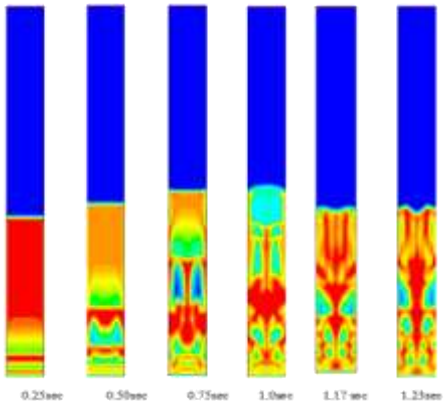

Fig. 13: Fluidization of solids

1) Volume fraction of air

Figure 14 shows the contours of volume fraction of air where blue color indicates low volume fraction of air and red color shows the maximum volume fraction of air. Wherever blue color is present it indicates air is less and solids are present at that spot. And red color indicates there is no solid at that spot.

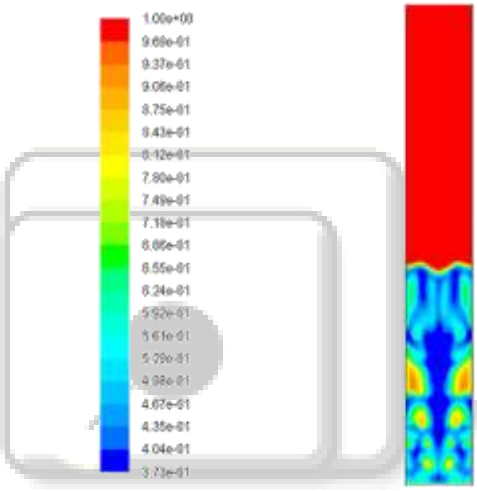

Fig. 14: The volume fraction of air in fluidized bed after fluidization.

2) Temperature Contours of Water

From fig15, it is observed that temperature of water sprayed initially is at 315k.Water moves from top to bottom, temperature reduces gradually till the bottom of bed and at the bottom of the bed is 298k to 299k.

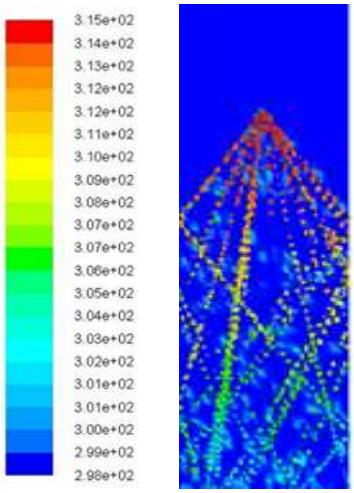

Fig. 15: Water temperature distribution as it passes through the fluidized bed.

3) Pressure Contours

Following Figure 16 shows the total pressure contour of 400 mm bed height. From fig it is seen that at the bottom of bed maximum pressure is noted which of the order of $5.52X10^3$ Pa. As bed height increases, gradually pressure decreases from $5.52X10^3$pa to $2.76X10^2$ pa and it reaches a constant pressure value of $5.52X10^3$ till the of the bed column. The average pressure at the Inlet is 5250 Pascal and at the outlet average pressure is 0.00817 Pa. This gives a pressure drop of 5250 Pa

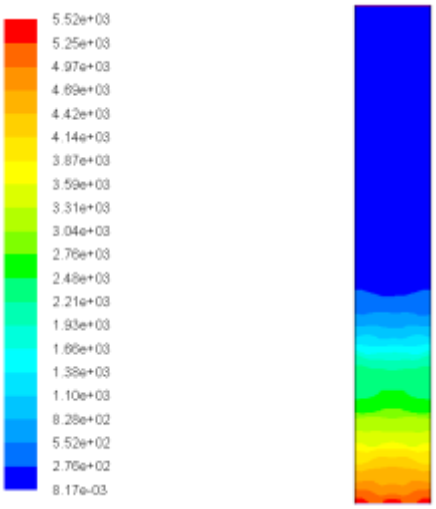

Fig. 16: Pressure distribution for static bed height of 400 mm.

VI. CONCLUSIONS

It is also observed that analysis of dynamic thermal parameters and heat transfer with respect to time is quite complex task.

Analysis of various parameters of different height fluidized bed, the following conclusion have been drawn:

1) As bed height increases, the time taken for fluidization increases.
2) Pressure drop is maximum for 400 mm bed height as compared to 300 mm and 200 mm since pressure drop increases with increase of bed height.
3) In all cases maximum pressure is found at the bottom of bed and gradually decreases with increase in height.
4) Temperature contours reveals that, as water moves from top to bottom of bed it loses its heat.
5) From temperature contours and pressure contours it is found that bed height of 300 mm gives appreciate performance since pressure drop is less compared to bed height of 400 mm and temperature difference is same.

REFERENCES

[1] Bigot, V., Guyot I. Bataille D., Roustan M., "Possibilities of use of two sensors depression metrological techniques and fiber optics, to characterize the hydrodynamics of a fluidized bed triphasic", In: Stork, A., Wild, G. (Eds.), Recent Advances in Process Engineering, vol. 4 (1990). pp. 143-1
[2] L. S. Fan, Gas–Liquid–Solid Fluidization Engineering, Butterworth-Heinemann, Boston, 1989
[3] V.K. Bhatia and N. Epstein, "Three-phase fluidization: a generalized wake model ", In: H. Angelino, J.P.

Couderc, H. Gibert and H. Lagueric, Editors, "Proceedings of the International Symposium on Fluidization, Its Application", Cepadues-Editions, Toulouse (1974), pp. 380–392

[4] Vishwanath M et al " Experimental and Numerical Analysis for Performance of Fluidized Bed Cooling Tower" International Journal of Engineering Research & Technology (IJERT)

[5] Advanced fluid dynamics book by anderson

[6] Shih th, liou ww, shabbir a, yang z, zhu j." a new k–ε eddy viscosity model for high reynolds number turbulent flows—model development and validation", comput fluids 24 (1995), 227–38

[7] Professor dengler "novel gas-liquid contacting operation that holds huge potential for large flow volumes transfer" " International Journal of Engineering Research & Technology (IJERT)

[8] V.K. Bhatia and N. Epstein, "Three-phase fluidization: a generalized wake model ", In: H. Angelino, J.P. Couderc, H. Gibert and H. Lagueric, Editors, "Proceedings of the International Symposium on Fluidization, Its Application", Cepadues-Editions, Toulouse (1974), pp. 380–392

[9] H.M. Jena, G.K. Roy, K.C. Biswal, "Studies on pressure drop and minimum fluidization velocity of gas–solid fluidization of homogeneous well-mixed ternary mixtures in un-promoted and promoted square bed", Chemical Engineering Journal 145 (2008) 16–24

[10] Rigby G.R., VanBrokland G.P., Park W.H., Capes C.E. "Properties of bubbles in three-phase fluidized bed as measured by an electro resistivity probe", Chemical Engineering Science 25 (1970), 1729–1741

[11] Larachi F., Cassanello M., Chaouki J., Guy C. "Flow structure of the solids in a 3-D gas–liquid–solid fluidized bed." A.I.Ch.E.Journal42 (1996), 2439–2452.

